

Elastic and Inelastic Photoproduction and Electroproduction of the J/ψ Particle

Senior Thesis by:
Allison Leich

Advisor: K. Griffioen

Coordinator: G. L. Hoatson

The College of William and Mary
April, 2009

Abstract

All available data on elastic and inelastic J/ψ photoproduction and electroproduction have been compiled and fit to simple parameterizations. These data span the range in center-of-mass energy W from threshold to 290 GeV. Fits using only a few parameters are possible for the total cross section vs. the center-of-mass energy. For elastic photoproduction, the χ^2 value of the fit was 1.9. For Inelastic photoproduction, the χ^2 value was 2.4. The inelastic photoproduction data have fractional energies $z < 0.9$. In the case of elastic electroproduction, the total cross section vs. center-of-mass energy was fit for three Q^2 bins covering the ranges 2 - 5 GeV², 5 - 10 GeV², and 10 - 100 GeV².

I. Introduction

1.1 Overview

The J/ψ particle is a meson of mass 3.097 GeV composed of a charm and an anti-charm quark. This mass is approximately three times that of a proton. Because the mass of the charm quarks is a substantial fraction of the total J/ψ mass, this system can be studied via non-relativistic quantum mechanics. The J/ψ is the lowest energy state of a charm anti-charm pair.

The quantum numbers of the J/ψ are equivalent to those of a photon. The projection of a photon's angular momentum along its direction of motion is ± 1 , and its total angular momentum (spin) is 1. According to Quantum Field Theory, a photon can fluctuate into a virtual quark-antiquark pair that has the same quantum numbers as the photon. Because this quark-antiquark pair is virtual, it will exist only for a short time before fluctuating back into a photon, as described by the Heisenberg Uncertainty Principle. If the quark pair interacts with a proton by the exchange of gluons, however, the quark pair can be given an energy boost sufficient to form a J/ψ particle. In laboratory experiments, the J/ψ is identified by its decay into a $\mu^+ \mu^-$ or $e^+ e^-$ pair. Figure 1 depicts how a photon, through proton interaction, fluctuates into a charm anti-charm pair, becomes a J/ψ , and then decays into a $\mu^+ \mu^-$ pair. The J/ψ can decay into $\mu^+ \mu^-$ or $e^+ e^-$ pairs, each with a $6.012 \pm 0.19\%$ probability.

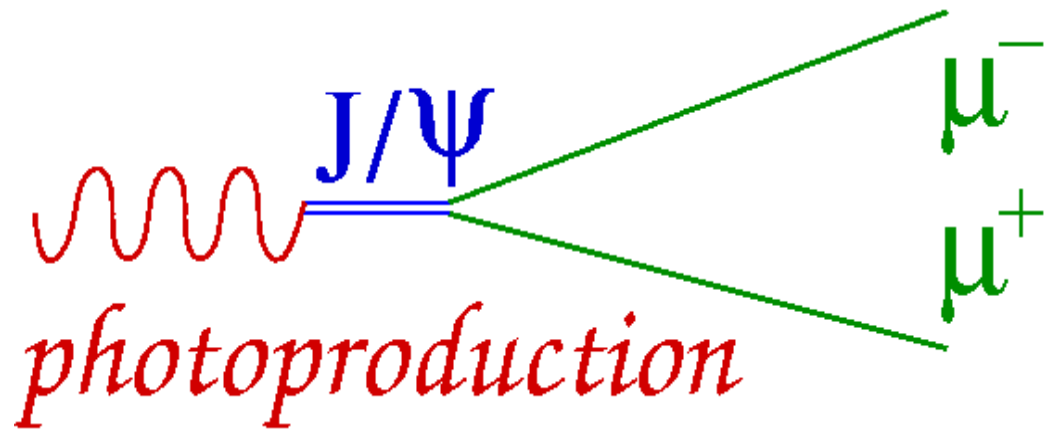


Figure 1. Photoproduction, in which an incoming photon forms a J/ψ , then decays into a μ^+, μ^- pair.

1.2 Discovery

The J/ψ particle was discovered in 1976 concurrently by Samuel C.C. Ting at the Brookhaven National Laboratory and by a group at the Stanford Linear Accelerator Center. Led by Burton Richter, the SLAC group named their discovery the ψ particle [11]. Ting named his discovery the J particle [12,25].

The term J/ψ was thus chosen in honor of both parties. The J/ψ particle was specifically discovered in the collision of electron and positron beams [11].

When a quark anti-quark pair is formed, the quarks travel in different directions until the strong force, which increases as their distance increases, pulls them back together. Figure 2 shows the J/ψ cross section versus the center-of-mass energy of the electron and positron. The J/ψ production is illustrated along the left

column. The right column depicts ψ' production. The top box represents data from the production of light hadrons; the middle box exhibits data from the decay mode of $\mu^+ \mu^-$. The bottom box illustrates decay into $e^+ e^-$. The resonance in Figure 1 indicates that a new particle has been formed [11]. If the four momenta of both of the decay particles observed is measured and added, the 4-vector dot product should reveal the squared mass of the J/ψ : 3.097 GeV, calculated as follows:

$$(E, p_x, p_y, p_z) \bullet (E, p_x, p_y, p_z):$$

$$E^2 = \vec{p}^2 + m^2 :$$

$$m^2 = E^2 - p_x^2 - p_y^2 - p_z^2$$

One therefore knows that a J/ψ has been formed when the added 4-momentum squared of the decay modes gives a peak at 3.097 GeV: The broadness of the resonance peaks demonstrates a variability in the cross section of a collision that created a J/ψ . Clearly, the highest probability of forming a J/ψ existed at the center-of-mass energy 3.097 GeV, yet the statistical probability of its formation is not zero on either side of this value.

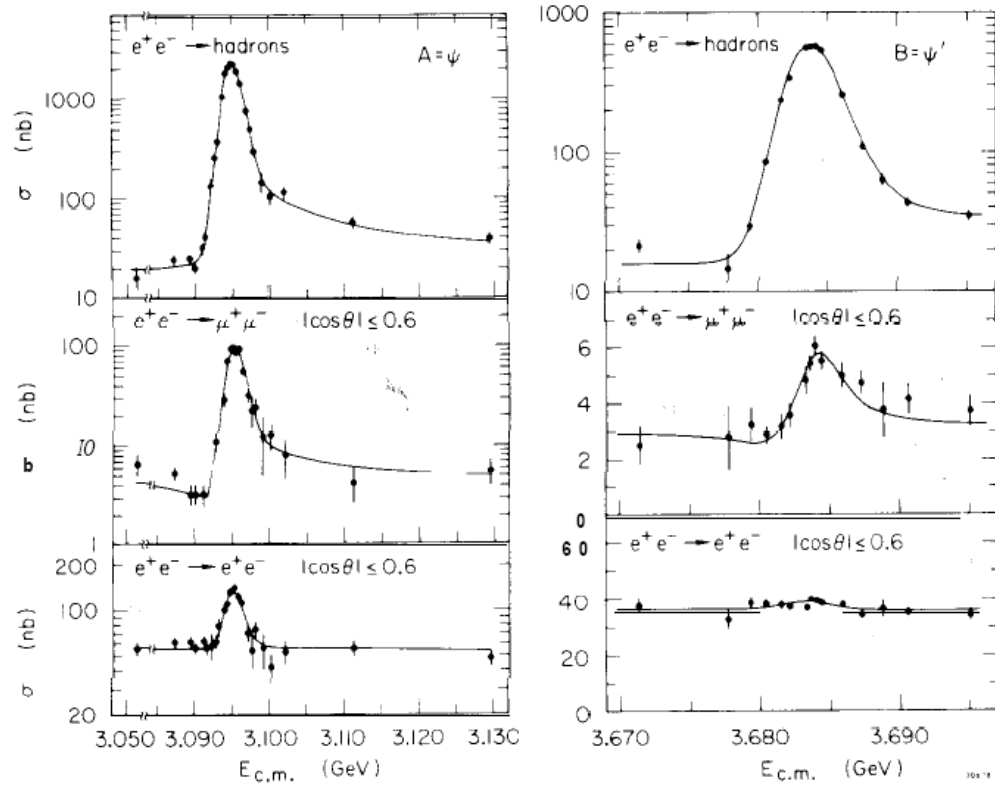


Figure 2. J/ψ production from e^+e^- collisions for J/ψ and ψ' . [11]

1.3 Specifications

The cross section can be visualized as follows: A particles is fired at a box containing many spheres. It is of interest to determine the likelihood of the particle scattering from one of the spheres in the box. Of course, as the size of these spheres increases, the likelihood that the particle will collide with one increases. Cross Section is essentially a measurement of statistical probability, describing the area taken up by the targeted spheres divided by the area of the box, where the box represents the bounds of the target hit by the incoming beam.

'W' shall be defined as the center of mass energy of the photon/proton system. The fractional energy z of a produced hadron h is given by

$$z = \frac{E_h}{\nu}, \quad (1)$$

in which E_h is the hadron energy and ν is the energy of the photon. The energy E_h must all come from the photon, so z cannot be larger than 1, but must be greater than 0.

Q^2 is the negative four-momentum squared of the photon:

$$Q^2 = q^2 - \nu^2 \quad (2)$$

The photon momentum, q , is equal to its energy ν in photoproduction, but not in electroproduction. Q^2 is equal to 0 for real photons, but is greater than 0 for virtual photons. In electroproduction, a virtual photon is emitted from the electron which mediates the reaction with a proton target. For the electroproduction data, Q^2 ranges from 2 to 100 GeV². In many papers, when Q^2 is approximately 0, this is denoted as the 'quasi-real' photon region, and the data are often referred to as photoproduction. The variable W_{TH} is defined as the threshold center-of-mass energy for the inelastic and elastic photoproduction of the J/ψ particle.

The program Root has been used to graph and fit the data. This program was written at the Organisation Européenne pour la Recherche Nucléaire (CERN) by high-energy physicists using C++. [13]

Papers on J/ψ photo- and electroproduction were found using the Spires-HEP database. This is a “High Energy Physics Literature Database” [14]. Upon retrieving papers, the numerical values were obtained from the HEPDATA reaction database [15]. References [20] and [21] provided explanations of the intricacies of this subject matter, thus facilitating the analysis process.

2. Data

2.1 Elastic Photoproduction

In the case of elastic photoproduction on a proton target, the collision produces a J/ψ and a proton, where the proton remains at its ground state. Here, the proton takes only a little energy in recoil. In searching for elastic photoproduction data, I expected to find Q^2 values at or very close to zero, indicating the production of real or quasi-real photons. In this elastic case, $W_{TH}^2 = 16.28 \text{ GeV}$. (W_{TH} is calculated via Equation 3, where M_P is the mass of a proton, 0.938 GeV).

$$W_{TH}^2 = M_{\psi} + M_P \quad (3)$$

Figure 3 shows the world's data for the elastic J/ψ photoproduction cross section as a function of W . As expected, there is no cross section below W_{TH} . Of course, as the cross section decreases along the 'y' axis, the probability of a production considerably decreases. The J/ψ can thus not be produced below a specific W . Above threshold, the cross section appears to increase significantly. On a log-log plot a power law

$$y = ax^\alpha \quad (4)$$

becomes

$$\ln(y) = \ln(a) + \alpha \ln(x) \quad (5)$$

if the natural log is taken of both sides. Equation 5 is the equation for a straight line of $\ln(y)$ versus $\ln(x)$. The equation for the fit of the elastic photoproduction plot (Figure 3) was constructed empirically by noticing the linear dependence of the cross section on a log-log plot. The data of σ vs. W were fit via Equation 6.

$$\sigma = a_1 \left(1 - \frac{W_{TH}^2}{W^2}\right)^{a_2} W^{a_3}, \quad W_{TH}^2 = 16.28 \text{ GeV}^2 \quad (6)$$

As evident by Equation 6, the exponential term in parentheses becomes zero at threshold, and the cross section simply depends upon a_1 and W^{a_3} at high W . Ref. [18] presented data from inelastic and elastic photoproduction of the J/ψ . The mean photon energy was 90 GeV. Ref. [2] presented data for σ and W from elastic J/ψ photoproduction. Data from Ref [1] come from Fermilab, showing elastic

photoproduction of J/ψ . The photon energy range was 100 to 375 GeV. Ref. [5] presents σ and W values for inelastic and elastic photoproduction of the J/ψ . Ref. [16] presents six additional points from which σ and W can be calculated, as described by reference [9]. Ref. [3] presents cross sections from proton positron collisions. Ref. [7] presents data for the production of J/ψ from $e^+ p$ collisions for which W ranged from 40 to 140 GeV, and the mean Q^2 value was 0.00005 GeV^2 . The data in Figure 3 include both $\mu^+ \mu^-$ and $e^+ e^-$ decay channels. Ref. [24] gives data for electron or positron collisions in which a J/ψ particle was formed by electroproduction and photoproduction. The elastic photoproduction data are plotted below, while the electroproduction data from this paper will be referenced later in the electroproduction discussion of Section 2.3. Data were compiled in both $\mu^+ \mu^-$ and $e^+ e^-$ decay channels.

The references [4] and [17] each contribute one datum in W . The W value was calculated using Equation 7.

$$W = \sqrt{2E_\nu M_p + M_p^2} \quad (7)$$

In this plot for elastic photoproduction, the χ^2 value was decent at 1.913. Equation 5 appears to sufficiently present the distribution of σ vs. W .

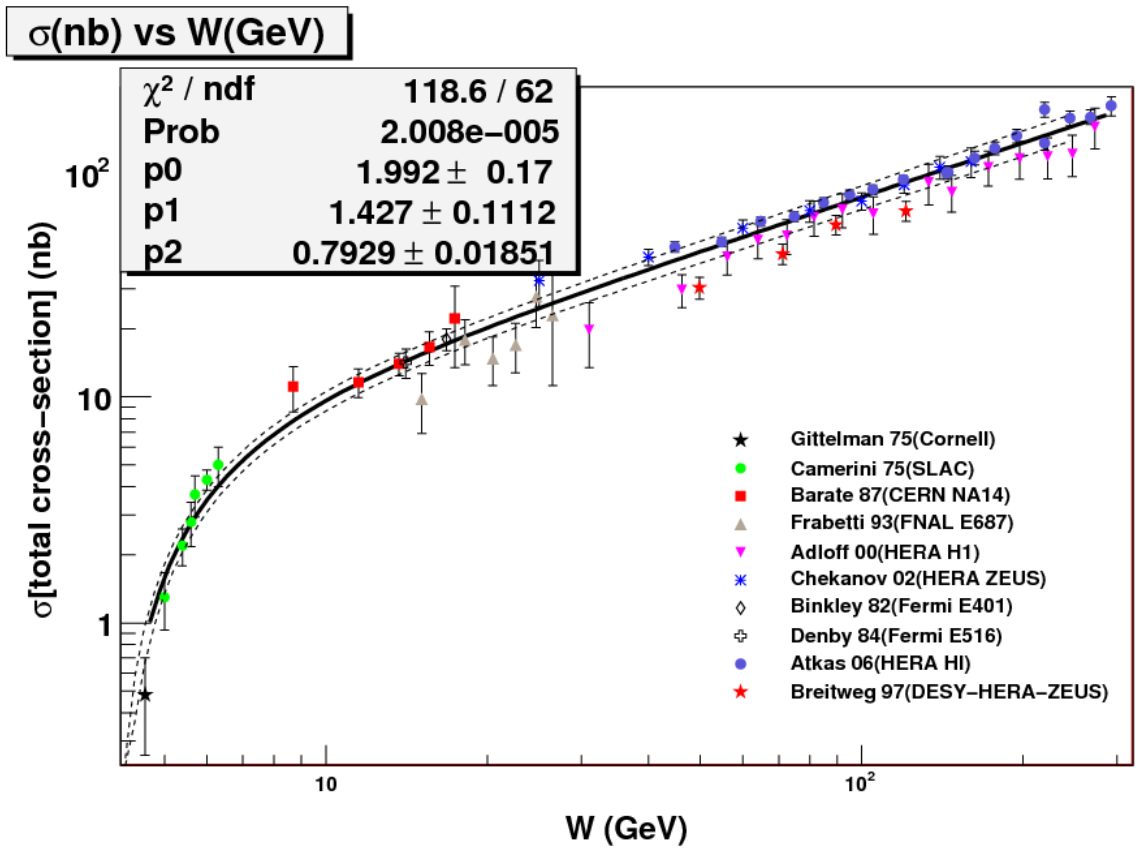


Figure 3. Elastic J/ψ production. The total cross section is plotted vs. the center-of-mass energy W . The parameters p_0 , p_1 , and p_2 correspond to a_0 , a_1 and a_2 in Equation 6.

Table 1: Data for elastic J/ψ photoproduction (The cross section σ includes statistical errors, followed by systematic errors when applicable.)

W(GeV)	σ (nb)	Reference
4.6	$0.48 \pm .22$	[17]
5	$1.3 \pm .37$	[16]
5.4	$2.2 \pm .41$	[16]
5.6	$2.8 \pm .62$	[16]
5.7	$3.7 \pm .76$	[16]
6	$4.3 \pm .44$	[16]
6.3	5 ± 1	[16]
8.7	11.1 ± 2.5	[18]
11.5	11.6 ± 1.7	[18]
13.7	14 ± 1.6	[18]
15.6	16.6 ± 2.8	[18]
17.4	22.2 ± 8.7	[18]
15.1	$9.8 \pm 2.9 +1.1 -1.2$	[1]
18.2	$17.9 \pm 4 +1.5 -3.0$	[1]
20.5	$14.8 \pm 3.6 +1.3 -2.6$	[1]
22.6	$17 \pm 4.2 +1.6 -3.2$	[1]
24.7	$27.8 \pm 7.5 +2.4 -3.8$	[1]
26.5	$23 \pm 11.8 +1.8 -3.6$	[1]
31	$19.8 \pm 6.3 \pm 5.1$	[2]
46.2	$29.8 \pm 5 \pm 3.4$	[2]
56.1	$41.7 \pm 7.1 \pm 4.8$	[2]
64	$49.5 \pm 8.7 \pm 5.6$	[2]
72.5	$51.8 \pm 9.1 \pm 5.9$	[2]
81.5	$62.4 \pm 11.1 \pm 7.1$	[2]
92	$67.6 \pm 11.7 \pm 7.7$	[2]
105.2	$64.6 \pm 12.1 \pm 7.4$	[2]
133.4	$89 \pm 18.3 \pm 12.7$	[2]
147.3	$80.6 \pm 15 \pm 12.7$	[2]
172.2	$104 \pm 18.2 \pm 16.4$	[2]
197.1	$113.6 \pm 21.7 \pm 18.0$	[2]
222.4	$116 \pm 23.7 \pm 18.5$	[2]
247.4	$118.9 \pm 24.6 \pm 19.0$	[2]
272.4	$156.9 \pm 32.2 \pm 25.0$	[2]
25	$32.6 \pm 7.5 \pm 5.2$	[3]
40	$41.5 \pm 3.5 \pm 3.3$	[3]
60	$55.8 \pm 4.8 \pm 4.6$	[3]
80	$66.6 \pm 7.3 \pm 7.0$	[3]
100	$73.4 \pm 6.4 \pm 6.0$	[3]
120	$86.7 \pm 7.2 \pm 6.5$	[3]

140	$104 \pm 12.1 \pm 11.0$	[3]
160	$110 \pm 16.3 \pm 12.0$	[3]
16.8	18 ± 2	[4]
14.1	14.2 ± 2.1	[5]
44.8	$46 \pm 2.4 \pm 4.0$	[24]
54.8	$48.5 \pm 2.3 \pm 4.3$	[24]
64.8	$59.7 \pm 2.8 \pm 5.3$	[24]
74.8	$62.7 \pm 3.2 \pm 5.5$	[24]
84.9	$72.6 \pm 3.4 \pm 6.4$	[24]
94.9	$78.6 \pm 3.7 \pm 6.9$	[24]
104.9	$82.6 \pm 4 \pm 7.3$	[24]
119.5	$91.5 \pm 3.5 \pm 8.1$	[24]
144.1	$98.3 \pm 4.4 \pm 8.7$	[24]
144.9	$98.6 \pm 6.6 \pm 9.6$	[24]
162.5	$114 \pm 8 \pm 12.0$	[24]
177.3	$126 \pm 8 \pm 15.0$	[24]
194.8	$143 \pm 10 \pm 25.0$	[24]
219.6	$187 \pm 14 \pm 18.0$	[24]
219.6	$133 \pm 10 \pm 17.0$	[24]
244.8	$171 \pm 13 \pm 17.0$	[24]
267.2	$173 \pm 13 \pm 18.0$	[24]
292.3	$194 \pm 19 \pm 23.0$	[24]
49.8	$30.4 \pm 3.4 \quad 3.6 - 5.4$	[7]
71.2	$42.9 \pm 4.5 \quad +4.9 - 6.0$	[7]
89.6	$57.7 \pm 5.8 \pm 7.4$	[7]
121	$66.5 \pm 6.8 \quad +9.2 - 11.2$	[7]

2.2 Inelastic Photoproduction

In inelastic photoproduction of the J/ψ , the initial proton leaves in an excited state. Here, the proton actually takes away energy by being excited. The data from Ref. [18] were cross sections for positron-proton collisions. W ranged from 50 GeV to 180 GeV, and z ranged from 0.1 to 0.9. Ref. [5] which showed up in the elastic photoproduction discussion of Section 2.1, also had inelastic data. Ref. [7] was also applicable here, presenting data for inelastic photoproduction of the J/ψ from $e^+ p$ collisions, where Q^2 was 0.00005 GeV^2 . Ref. [6] gives values from electron-positron collisions for W from 60 GeV to 160 GeV, where Q^2 is approximately 0, thus small enough to deem the photons real as opposed to virtual. Ref. [26] presents one additional point from which σ and W can be calculated, as described by reference [9]. Ref. [8] gives combined cross sections for $e^+ e^-$ and $\mu^+ \mu^-$ decay channels. Ref. [19] presents data from electron or positron beams at 27.5 GeV where W ranged from 30 to 220 GeV. Again, the total cross section (nb) is plotted vs. the center-of-mass energy in GeV. The data were fit via Equation 9, which is the same form used in the elastic photoproduction case. The W_{TH}^2 value in this inelastic case was calculated to be 17.42, a slight deviation from the elastic case, with the addition of the mass of a pion at 0.139 GeV:

$$W_{\text{TH}}^2 = M_{\psi} + M_p + M_{\pi} \quad (8)$$

Of course, W_{TH}^2 is larger than in the elastic case because the emergent excited proton must decay into at least a nucleon plus a pion.

$$\sigma = a_1 \left(1 - \frac{W_{TH}^2}{W^2}\right)^{a_2} W^{a_3}, \quad W_{TH}^2 = 17.42 \text{ GeV}^2 \quad (9)$$

Figure 4 shows the data for inelastic photoproduction of the J/ψ meson. Although the fit is good, it should probably slope upward more steeply near threshold, then continuing linearly upwards at higher W . Clearly, the greatest discrepancies exist among the various experiments at higher W values. This plot gave a decent χ^2 value of 2.446, despite the systematic differences in the data sets.

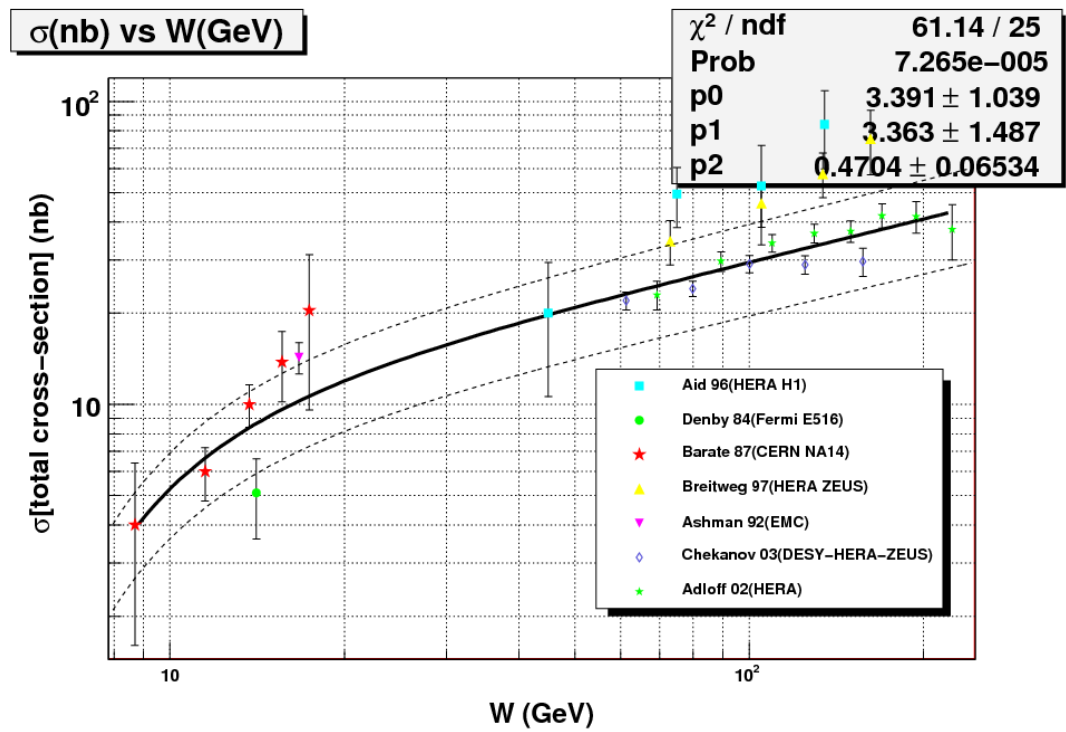


Figure 4. Inelastic photoproduction. The total cross-section vs. center-of-mass energy W is depicted. Parameters are defined as in Figure 3.

Table 2: Data for inelastic J/ψ photoproduction (The cross section σ includes statistical errors, followed by systematic errors, when applicable.)

W(GeV)	σ (nb)	Reference
8.7	4 ± 2.4	[18]
11.5	6 ± 1.2	[18]
13.7	10 ± 1.6	[18]
15.6	13.8 ± 3.6	[18]
17.4	20.4 ± 10.8	[18]
14.1	5.1 ± 1.5	[5]
	$20 \pm 9.4 +3.2$	[8]
45		
	$49.5 \pm 11.1 \pm 7.9$	[8]
75		
	$52.6 \pm 19.0 \pm 8.4$	[8]
105		
135	$84.1 \pm 24.3 \pm 13.4$	[8]
	$34.6 \pm 5.8 +4.0 -3.1$	[7]
73		
	$46.1 \pm 7.6 +3.6 -2.2$	[7]
105		
	$57.8 \pm 9.7 +5.6 -3.0$	[7]
134		
	$75.3 \pm 18.1 +7.4 -6.9$	[7]
162		
16.7	14.3 ± 1.7	[26]
61.3	$22 \pm 1.5 +2.6 -2.9$	[19]
79.9	$24.1 \pm 1.4 \pm 2.2$	[19]
100.1	$29.1 \pm 1.9 +2.6 -3.5$	[19]
124.8	$28.9 \pm 2 +4.0 -3.2$	[19]
157.2	$29.6 \pm 3.2 +3.5 -3.0$	[19]
69.3	$23 \pm 2.5 \pm 3.2$	[6]
89.4	$29.7 \pm 2.2 \pm 4.1$	[6]
109.5	$34.1 \pm 2.3 \pm 4.7$	[6]
129.6	$36.7 \pm 2.6 \pm 5.1$	[6]
149.6	$37.3 \pm 3 \pm 5.2$	[6]
169.6	$42 \pm 3.9 \pm 5.8$	[6]
194.2	$41.7 \pm 4.9 \pm 5.8$	[6]
224.2	$37.8 \pm 7.8 +5.0 -5.9$	[6]

2.3 Electroproduction

Data for J/ψ electroproduction were also compiled. The drive to measure J/ψ production via electroproduction stems from the ability to manipulate the virtual photon's wavelength without changing its energy. In the case of real photons, energy and momentum are tied, and the wavelength cannot be manipulated independent of the energy of the photon. Stated another way, for electroproduction, $v \neq q$.

Using Ref. [10], I have taken data for the cross sections of J/ψ electroproduction as functions of W and Q^2 from 2 - 5, 5 - 10², and 10 - 100 GeV². The various experiments referenced in this study used slightly different Q^2 bins. Therefore, the three fits in Figure 5 assume approximate Q^2 bins of 2 to 5 GeV², 5 to 10 GeV², and 10 to 100 GeV². Deviations from these ranges will be stated. Ref. [23] presents data for σ (virtual photon-proton cross section) as a function of W in Q^2 bins 2-6, 6-18, and 18-80 GeV². The data in the 2-6 GeV² range were fit in the 2-5 GeV² category, as the mean Q^2 value was 3.5 GeV². The data from 6-18 and 18-80 GeV² were placed in the 10-100 GeV² category, where the average Q^2 values were 10.1 GeV² and 33.6 GeV², respectively. These points appear to complement the other data points in the highest Q^2 region. Ref. [22] gives W and σ values for Q^2 bins 2-7 and 7-40 GeV². The data for Q^2 from 2-7 GeV² were plotted in the 2-5 GeV² bin. The average Q^2 value for this set of data was 3.5 GeV². Upon examination of the plot, these values appear to stray from Ref. [24] and Ref. [10] in the 2-5 GeV² range. The error bars on the data in Ref. [22], however, are significant. The data for 7-40 GeV² were placed in the 10-100 GeV² category. These

points seem to fit in this bin. The data from Ref. [24] are for electron or positron beams in which a J/ψ particle was formed by electroproduction. Values of σ are given for various values of W and for Q^2 bins of 2-5, 5-10, and 10-80 GeV^2 . Equation 6 was used to fit the data points, with the same W_{TH} as was used for elastic photoproduction. The fit appears sufficient to characterize the dependence of σ and W on Q^2 . The parameters for the three Q^2 bins are: $a_0 = 1.26138$, $a_1 = 1.9665$, $a_2 = 0.733671$ (2 to 5 GeV^2), $a_0 = 0.526598$, $a_1 = -26.693$, $a_2 = 0.788624$ (5 to 10 GeV^2), and $a_0 = 4.92\text{E-}6$, $a_1 = -334.361$, $a_2 = 2.86116$ (10 to 100 GeV^2).

Elastic Electroproduction

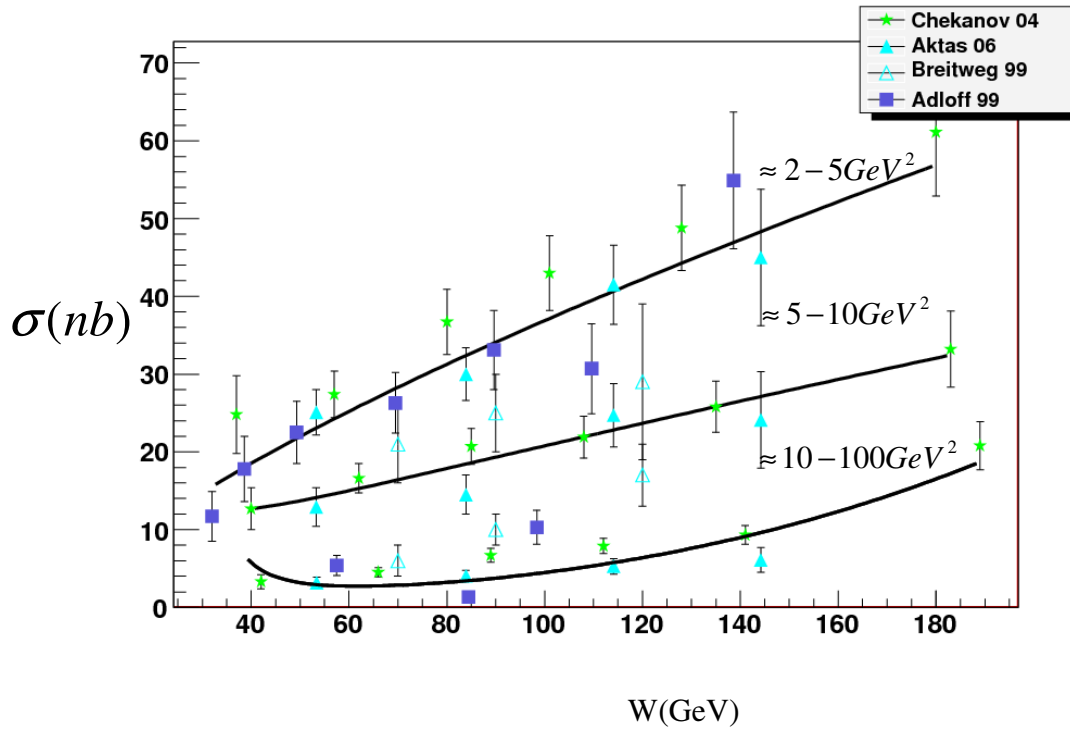


Figure 5. Total cross sections for elastic electroproduction vs. center-of-mass energy for three Q^2 regions, $\approx 2-5 GeV^2$, $\approx 5-10 GeV^2$, and $\approx 10-100 GeV^2$.

Table 3: Data for elastic J/ψ electroproduction (The cross section σ includes statistical errors, followed by systematic errors, when applicable.)

W(GeV)	σ (nb)	Q^2 (GeV ²)	Reference
37	24.8 ± 5.0 +5.6,-6.6	2-5	[10]
57	27.4 ± 3.0 +3.1, -3.9	2-5	[10]
80	36.7 ± 4.2 +10.5, - 3.0	2-5	[10]
101	43.0 ± 4.8 +3.0, -4.5	2-5	[10]
128	48.8 ± 5.5 +9.0, -4.3	2-5	[10]
180	61.1 ± 8.2 +11.5, -5.1	2-5	[10]
40	12.7 ± 2.7 +3.9 -1.9	5-10	[10]
62	16.6 ± 1.9 +2.9 -1.3	5-10	[10]
85	20.7 ± 2.3 +1.6 -1.4	5-10	[10]
108	21.9 ± 2.7 +1.1 -0.7	5-10	[10]
135	25.8 ± 3.3 +1.1 -1.3	5-10	[10]
183	33.2 ± 4.9 +4.5 -1.4	5-10	[10]
42	3.3 ± 0.9 +0.8 -1.0	10-100	[10]
66	4.5 ± 0.6 +1.4 -0.4	10-100	[10]
89	6.7 ± 0.9 +0.9 -1.4	10-100	[10]
112	7.9 ± 1.0 +0.4 -1.2	10-100	[10]
141	9.3 ± 1.2 +2.1 -0.8	10-100	[10]
189	20.8 ± 3.1 +1.7 -1.2	10-100	[10]
53.3	25.1 ± 2.9 ± 2.4	2-5	[24]
89.9	30 ± 3.4 ± 2.9	2-5	[24]
114.1	41.5 ± 5.1 ± 4.0	2-5	[24]
144.2	45 ± 8.8 ± 4.5	2-5	[24]
53.3	12.9 ± 2.5 ± 1.2	5-10	[24]
89.9	14.5 ± 2.5 ± 1.4	5-10	[24]
114.1	24.7 ± 4.1 ± 2.4	5-10	[24]
144.2	24.1 ± 6.2 ± 2.5	5-10	[24]
53.4	$3.19 \pm .69$ ± 0.31	10-80	[24]
83.9	$4.04 \pm .7$ ± 0.39	10-80	[24]
114.1	5.29 ± 1 ± 0.5	10-80	[24]
144.2	6.10 ± 1.6 ± 0.6	10-80	[24]
32	11.7 ± 3.2 ± 2.9	2-6	[23]
49.3	22.5 ± 4.0 ± 3.6	2-6	[23]
69.5	26.3 ± 3.9 ± 4.2	2-6	[23]
89.6	33.1 ± 5.1 ± 5.2	2-6	[23]
109.6	30.7 ± 5.8 ± 4.8	2-6	[23]
138.6	54.9 ± 8.9 ± 8.8	2-6	[23]

57.5	$5.4 \pm 1.3 \pm 0.9$	6-18	[23]
98.4	$10.3 \pm 2.2 \pm 1.7$	6-18	[23]
138.6	$17.8 \pm 4.2 \pm 3.1$	6-18	[23]
84.4	$1.34 \pm 0.37 \pm 0.24$	18-80	[23]
70	$21.0 \pm 5 \pm 3$	2-7	[22]
120	$29.0 \pm 10 \pm 6$	2-7	[22]
90	$25.0 \pm 5 \pm 4$	2-7	[22]
70	$6.0 \pm 2 \pm 1$	7-40	[22]
120	$17.0 \pm 4 \pm 3$	7-40	[22]
90	$10.0 \pm 2 \pm 2$	7-40	[22]

III. Conclusions

The world's data on elastic and inelastic J/ψ photoproduction and electroproduction can be fit to simple parameterizations. Equations 6 and 9 successfully fit the data for elastic and inelastic photoproduction of the J/ψ particle. In the fit to elastic photoproduction, the χ^2 value was decent, at 1.913. In the case of inelastic photoproduction, the fit gave a χ^2 value of 2.446. In the case of elastic electroproduction, the total elastic cross section vs. the center-of-mass energy was plotted and fit for the approximate bins Q^2 of 2 to 5, 5 to 10, and 10 to 100 GeV^2 . The data from the four sources for various Q^2 bins are reasonably well-described by the fit. This data analysis should be continued in the future, in order to obtain a model for electroproduction in terms of the independent variables Q^2 , W , and z , based on the parameters given in Section 2.3.

References

1. P.L. Frabetti, *et al.*, Phys. Lett. **B316**(1993)197.
2. C. Adloff, *et al.*, Phys. Lett. **B483**(2000)23.
3. S. Chekanov, *et al.*, Eur. Phys. J. **C24**(2002)345.
4. M. Binkley, *et al.*, Phys. Rev. Lett **48**(1982)2.
5. B. H. Denby, *et al.*, Phys. Rev. Lett **52**(1984)10.
6. C. Adloff *et al.*, H1 collaboration, hep-x(0205064).
7. J. Breitweg, *et al.*, Z.Phys. **C76** (1997)599.
8. S. Aid *et al.*, Nucl. Phys. **B472**(1996)3.
9. N. Baillie, R. Fersch, K. Griffioen “Inelastic and Elastic Cross Section Curve Fits For J/Psi photoproduction” 31 October, 2002
http://mail.google.com/mail/?ui=2&view=js&name=js&ver=Xz0jXTrYL5Y.en.&am=b7EopeS3cCFLDX3i1_Q2St-4gVqmqSQ.
10. S. Chekanov, *et al.* DESY-HERA-ZEUS NP **B695** (2004)3.
11. ¹ Burton Richter http://nobelprize.org/nobel_prizes/physics/laureates/1976/richter-lecture.pdf December 11, 1976 Stanford University, Stanford California pg. 9.
12. Brookhaven National Laboratory.
http://www.bnl.gov/bnlweb/history/Nobel/Nobel_76.asp.
13. <http://root.cern.ch/drupal/>.
14. <http://www.slac.stanford.edu/spires/>.
15. HEPDATA: REACTION DATA Database, <http://durpdg.dur.ac.uk/>.
16. U. Camerini, *et al.*, Phys. Rev. Lett **35**(1975)483.
17. B. Gittelman, *et al.*, Phys. Rev. Lett **35**(1975)1616.
18. R. Barate, *et al.*, Z. Phys. **C33**(1987)505.
19. Chekanov, *et al.*, EPJ **C27**,173(2003).
20. N. P. Zotov, I.I Katkov, A.V. Lipatov, Physics of Atomic Particles Vol.69, No. **12**(2045-2055).
21. H. G. Dosch, E. Ferreira Physics Lett **B-576** (2003) 83–89.
22. J. Breitweg *et al.*, ZEUS COLLABORATION Eur. Phys. J. **C6** (1999)603.
23. C. Adloff, *et al.*, Eur. Phys. J **C10**(1999)373.
24. Aktas, *et al.*, Eur. Phys. J **C46**(585).
25. S. C. C. Ting (MIT, LNS) Jun 1976, 669-709.
26. J. Ashman *et al.*, Z.Phys **C56**(1999)21.